PHILOSOPHICAL TRANSACTIONS OF THE ROYAL SOCIETY A MATHEMATICAL, PHYSICAL & ENGINEERING SCIENCES

Controlling cold atoms above a magnetic reflector

E.A. Hinds

Phil. Trans. R. Soc. Lond. A 1999 **357**, 1409-1420
doi: 10.1098/rsta.1999.0381

THE ROYAL SOCIETY

Controlling cold atoms above a magnetic reflector

By E. A. Hinds

Sussex Centre for Optical and Atomic Physics, University of Sussex, Brighton BN1 9QH, UK

This article outlines the basic physical principles of the magnetic atom reflector and summarizes the state of experiments performed by our group. I also discuss several new ideas for extending the magnetic reflector to confine atoms to a plane, a wire or a dot. These ideas aim at the general problem of controlling atomic motion for use in atom optics. The two-dimensional gas provides a new system in which to study quantum statistical properties such as Bose–Einstein condensation and other phase transitions. The confinement of cold atoms to wires and dots leads naturally towards the realization of a quantum computer.

Keywords: atom optics; two-dimensional gas, trapped atoms; quantum computation

1. Introduction

Over the last few years, it has become possible to prepare extremely cold atomic vapours by means of laser cooling and trapping (Adams & Riis 1997). This has generated a surge of interest in techniques for manipulating atoms, and has given birth to the field of atom optics (Arimondo & Bachor 1996; Prentiss & Phillips 1997). One aim of atom optics is to make atoms and their associated de Broglie waves display the usual features of photon optics, including reflection, diffraction and interference. In addition, new effects are to be expected because atoms have mass and complex internal structures, features that photons are lacking. In my group, we have been investigating the possibilities for manipulating cold atoms by static magnetic and electric forces. The manipulation of atoms spans many topics of current interest. Some examples are the control of atomic trajectories for atom lithography (Timp *et al.* 1992; McClelland *et al.* 1993); the measurement of gravitational fields by atom interferometry (Berman 1997); the study of quantum statistics and Bose–Einstein condensation (Griffin *et al.* 1995); and quantum computation (Williams & Clearwater 1998).

Ever since the famous experiment of Stern & Gerlach (1922), it has been well established that atoms are deflected by the interaction of their magnetic moment with a magnetic field gradient. This Stern–Gerlach force has been important throughout the history of atomic and molecular beams, both as a means of state selection and as a way of focusing atoms (Ramsey 1985; Kaenders *et al.* 1995). The largest convenient interaction potential, for example one Bohr magneton in a magnetic field of 1 T, is only 60 μeV or 0.7 K. Because this is so small in comparison with thermal energy kT at room temperature, the Stern–Gerlach force has been restricted until very recently to the deflection of atomic beams through small angles, typically not much more than a degree. However, laser cooling techniques developed over the past 15 years can now

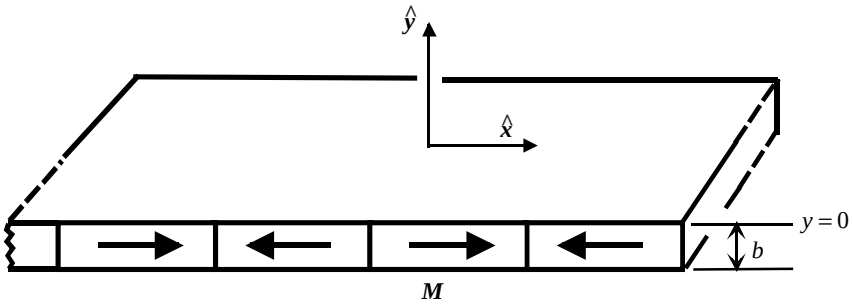

Figure 1. Schematic diagram of the mirror surface showing alternating magnetization $\boldsymbol{M}$ in the $\hat{\boldsymbol{x}}$-direction. Also shown are the normal to the surface, which defines the $\hat{\boldsymbol{y}}$-direction, the origin of the y-axis, and the thickness, b, of the magnetic layer. In our experiments $b = 3$ μm, and the period of the magnetization is typically in the range 1–10 μm.

refrigerate clouds of atoms to temperatures in the range 1 μK–1 mK, where thermal energy is dwarfed, even in comparison with quite modest magnetic interactions. Such clouds can be captured magnetically, using the Stern–Gerlach force, to produce not merely a small deflection but complete imprisonment of the atoms. Here, the gravitational force becomes an important consideration. For example, a 100 μK rubidium atom does not have enough energy to rise even 1 mm in the Earth's gravitational field. Thus, it is not sufficient for the confining potential merely to exceed the thermal energy, it must also provide a levitating force to cancel the weight. Fortunately, the required field gradient is a modest one, only 15 G cm^{-1} in the case of Rb.

Following a suggestion by Opat *et al.* (1992), our group was able, in 1995, to demonstrate a new kind of atomic mirror based on the Zeeman interaction between a ground-state atom and the field above a magnetized strip of audio tape (Roach *et al.* 1995), and subsequent refinements (Hughes *et al.* 1997*a*, *b*) have brought us to the point where high-resolution reconstruction of an atomic cloud is possible using a magnetic reflector. In this paper, I review the principles of the magnetic reflector and the state of experimental research. I also propose new extensions of the magnetic reflector in which it may be possible to trap cold atoms in a two-dimensional gas using combinations of static electric and magnetic fields. Such a trap has possible applications in the manipulation of single atoms, and the realization of ideas in quantum computing.

2. Principles of the magnetic mirror

An atom in a magnetic field of magnitude B, has the magnetic dipole interaction energy $U = -\mu_\zeta B$, where μ_ζ is the projection of its magnetic moment onto the field direction. Provided the magnetic field changes slowly enough (and it does for the cold atoms in our experiments), the magnetic moment follows the field adiabatically and the angle between them is constant. In this adiabatic regime, the potential energy of the atom depends on the field magnitude B, but not its direction. The field of our atomic mirror increases near the surface and μ_ζ is normally chosen to be negative so that the atom can be reflected by the Stern–Gerlach force $\nabla\mu_\zeta B$. This is the basic principle.

The static field $\boldsymbol{B}$ above a magnetic surface can be described by a scalar potential ϕ, related to the magnetization $\boldsymbol{M}(\boldsymbol{r}')$ within the material by eqn (5.100) of Jackson's

book (1975):

$$\phi(\boldsymbol{r}) = -\frac{\mu_0}{4\pi}\int_V \frac{\nabla'\cdot\boldsymbol{M}(\boldsymbol{r}')}{|\boldsymbol{r}-\boldsymbol{r}'|}\,\mathrm{d}^3r' + \frac{\mu_0}{4\pi}\oint_S \frac{\boldsymbol{n}'\cdot\boldsymbol{M}(\boldsymbol{r}')}{|\boldsymbol{r}-\boldsymbol{r}'|}\,\mathrm{d}^2r', \tag{2.1}$$

where V and S are the volume and surface area of the material, and $\boldsymbol{n}'$ is the normal to the surface. For our atomic mirrors, the direction of the magnetization is primarily parallel or anti-parallel to one axis, which we take to define $\hat{\boldsymbol{x}}$ as shown in figure 1. The surface of the mirror is flat with its normal $\boldsymbol{n}'$ defining the $\hat{\boldsymbol{y}}$-axis. With this geometry,

$$\phi(\boldsymbol{r}) = -\frac{\mu_0}{4\pi}\int_V \frac{\partial M/\partial x'}{|\boldsymbol{r}-\boldsymbol{r}'|}\,\mathrm{d}^3r'. \tag{2.2}$$

An additional feature of the mirror is that the magnetization is periodic, with a repetition length λ. Therefore, it is convenient to expand the magnetization in a Fourier series

$$M = \frac{1}{2}\sum_{n=0}^{\infty} M_n \mathrm{e}^{\mathrm{i}nkx'} + \text{c.c.}, \tag{2.3}$$

in which $k = 2\pi/\lambda$ and c.c. indicates the complex conjugate. Equation (2.2) then becomes

$$\phi(\boldsymbol{r}) = -\frac{\mu_0}{8\pi}\sum_n \mathrm{i}nk\int_V \frac{M_n \mathrm{e}^{\mathrm{i}nkx'}}{|\boldsymbol{r}-\boldsymbol{r}'|}\,\mathrm{d}^3r' + \text{c.c.} \tag{2.4}$$

In general, this integral cannot be evaluated analytically, however, Laplace's equation for $\phi(\boldsymbol{r})$, together with the periodicity of $\boldsymbol{M}$, impose a structure on the field of the form

$$\begin{pmatrix} B_x \\ B_y \end{pmatrix} = \mp\sum_n B_n \mathrm{e}^{-nky}\begin{pmatrix} \cos(nkx+\delta_n) \\ \sin(nkx+\delta_n) \end{pmatrix}, \tag{2.5}$$

in which B_n is the field amplitude of the nth harmonic at the surface of the mirror, and δ_n is the phase of the magnetization defined by $M_n = |M_n|\mathrm{e}^{\mathrm{i}\delta_n}$. We note that each harmonic in equation (2.5) decreases exponentially with distance from the surface, the longest range being associated with the fundamental. When the magnetization is constant throughout the thickness b of the material, one finds that

$$B_n = \tfrac{1}{2}(1-\mathrm{e}^{-nkb})\mu_0|M_n| \tag{2.6}$$

(Hughes *et al.* 1997*b*). This shows that the maximum field available to reflect atoms is only half the remanent field, and that if the wavelength of the magnetization is much greater than the thickness b of the magnetized layer, there is a further suppression given by the term in parentheses. These factors can be understood if we replace the magnetization of the material by an effective surface current per unit width of $\boldsymbol{M}\times\boldsymbol{n}'$. The field due to the current on the front surface is $\frac{1}{2}\mu_0|\boldsymbol{M}|$, but this is cancelled, in part, by the exponentially attenuated field from the surface current flowing on the back. If the direction of magnetization is along $\hat{\boldsymbol{y}}$ (out of plane) instead of $\hat{\boldsymbol{x}}$ (in plane), it is the surface integral of equation (2.1) that determines the magnetostatic potential. Nevertheless, after some work, the final result for the field strength is identical to equation (2.6).

In the simplest case, the magnetization is a pure sine wave, the magnitude B of the field is given by equation (2.5) as $B_1 e^{-ky}$, and, for an atom whose magnetic moment along the field is μ_ζ, the interaction energy is then

$$U = -\mu_\zeta B_1 e^{-ky}. \tag{2.7}$$

We see that for negative values of μ_ζ, the interaction is repulsive and has flat equipotentials: in short, it is a mirror. To give a sense of the energy scales, I note that a 15 G surface field is sufficient to reflect rubidium atoms in the ($5S_{1/2}$ $F = 3$, $m_F = 3$) ground state, dropped from a height of 1 cm. In our atomic mirror, the surface field is *ca.* 1 kG, and the attenuation length $1/k$ is typically 2 μm. For atoms dropped onto such a mirror, the reflecting potential is very steep compared with the gravitational one, and the atom turns around in a very short distance.

3. Experimental demonstration

Our group has recently performed an experiment in which a millimetre-sized cloud of several million cold ^{85}Rb atoms falling freely under gravity is brought to a focus by reflection from a horizontal concave magnetic atom mirror. We are now able to observe directly how the cloud evolves as it expands thermally and, for the first time, to reconstruct the original cloud by means of specular reflections. The reversibility of the atomic motion is made possible by the high quality of the mirror.

There were three essential experimental advances as follows.

(i) The sine wave (of wavelength $\lambda = 12$ μm) is recorded in a single 12 mm wide track across the full width of a half-inch video tape (Ampex 398 Betacam SP), rather than being pieced together from many different tracks on a floppy disk as it was previously.

(ii) The field B_1 at the surface of the tape is large, approximately 1 kG, which keeps the atoms away from the surface. In our experiments, the closest approach is $y = 6$ μm, where the factor e^{-ky} is 0.04. At this large distance from the surface the mirror is smooth because the nth harmonics are suppressed by factors of $(0.04)^n$, and only the fundamental frequency component remains significant.

(iii) We have developed a new method for producing curved mirrors. A short length of the tape is glued across the end of a thin-walled ceramic tube using high vacuum epoxy. A high-quality convex lens is pressed onto the tape, forcing it to be curved (radius $R = 54$ mm in this particular case). Epoxy poured into the back of the tube holds this shape when the lens is removed. Since the tape reflects light, we can study the surface quality in a Twyman–Green interferometer (Born & Wolf 1980) and we find that the surface figure is accurate to better than 4 μm over the central 8 mm.

The reflector is installed in a high vacuum chamber, pumped down to a pressure of 2×10^{-9} Torr†. A magneto-optical trap (Adams & Riis 1997) collects a small cloud 1 mm across containing several million ^{85}Rb atoms located on the optical axis 12 mm above the reflector. This particular height is close to one-quarter of the radius of curvature R, the focal plane of the mirror. In conventional optics, the light travels

† It is worth noting that all the recording media we have studied evolve remarkably little gas.

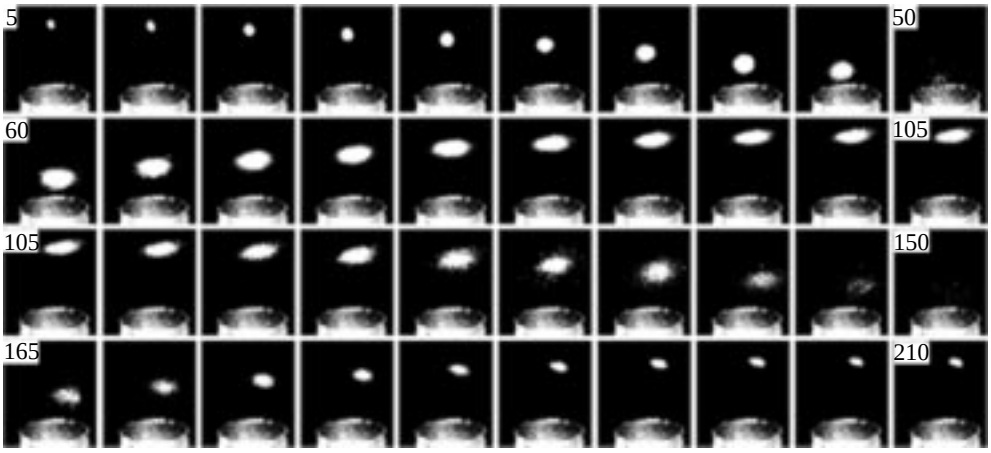

Figure 2. Motion of atoms bouncing on the magnetic reflector after release from height $\frac{1}{4}R$. The images of the atom cloud are formed by scattered laser light. Each frame is the average of ten acquisitions with a background subtracted. The magnetic reflector is seen at the bottom of each frame with the time delay shown in milliseconds. Upper strip: the cloud expands as it falls, but then rises with constant diameter after the first bounce from the surface. Between 45 ms and 55 ms, the cloud is below the laser beam used for detection and cannot be seen. Lower strip: the collimated cloud falls to the mirror for the second time and then rises to a focus that reconstructs the original cloud.

in straight lines giving a focal length of $\frac{1}{2}R$, but, here, the atoms fall under gravity on parabolic trajectories, resulting in a focus at $\frac{1}{4}R$ (Hughes *et al.* 1997*b*). After being released from the trap, the atoms are cooled by optical molasses (Adams & Riis 1997) for 20 ms, then optically pumped for 1 ms by a retro-reflected σ^+ light beam, which transfers the majority of them to the most favourable state for magnetic reflection ($F = 3$, $m_F = +3$). Now the cloud falls freely in the dark until we flash on the optical pumping beam once again, this time for detection purposes. The scattered photons are collected by a Princeton Instruments MicroMax768 CCD camera, which records a snapshot of the atom distribution at that time.

Figure 2 is a sequence of images taken with increasing time delays, viewed at a slight angle so that the surface of the magnetic reflector is visible at the bottom of each frame. The first row shows the cloud falling freely under gravity. Its diameter is determined partly by the original size and partly by the thermal expansion at 10 cm s^{-1} (FWHM) due to the cloud temperature of 18 μK. In the tenth frame, we see that the atoms have almost fallen out of the detection beam. Still, we know from the measured expansion rate that the cloud diameter must be 5 mm when it reaches the mirror (10 mm diameter), and we expect all but 5% of the atoms to be reflected. At 60 ms, the cloud reappears with just the width anticipated, and in the second row it rises to its original height without further expansion. This shows that the atoms are collimated, i.e. the atomic velocities are all vertical and the diameter of the cloud is determined by the thermal spread at the moment when it lands on the reflector. Although the original horizontal thermal velocity of each atom has been removed by its interaction with the reflector, that velocity remains encoded in the transverse position of the atom. In the third row of figure 2, the collimated atom cloud falls

back down towards the mirror. Once again, there are some frames where the cloud is too low to be seen, but at 165 ms it reappears after the second bounce. The final row shows the atoms coming to a focus in which the original cloud is eventually reconstituted. This happens because the second bounce imparts a transverse velocity to each atom that is just the reverse of its original thermal velocity. To our knowledge, this is the first example of a reversal, or 'echo', in the time evolution of such a complex ensemble. It is reminiscent of the spin echo technique (Hahn 1950), which reverses transverse decoherence in magnetic resonance. With careful analysis of the data, we find that there is a slight blurring of the image cloud. We do not yet know the origin of this but we note that the reversibility of the motion hinges on the absence of perturbations to the cloud in free flight, as well as on the high quality of the reflector itself.

This experiment demonstrates the geometrical optics of the concave atom reflector, and further direct measurements of this kind should make it possible to fabricate increasingly refined magnetic reflection surfaces for the high-resolution imaging of cold atoms. Ultimately, of course, the bouncing atoms must satisfy the Schrödinger equation and, if they are sufficiently coherent, should exhibit interference effects. From this point of view, the reflector in our experiment can be considered as a resonant cavity, closed physically at the bottom and by gravity at the top (Wallis *et al.* 1992). The motion we have observed is then reminiscent of a confocal cavity in which the waist size of the propagating beam alternates between large and small. In the present case, however, the longitudinal mode spacing is very much smaller than the thermal energy spread of the cloud, so many modes are occupied and the resonances cannot be detected. We are now aiming to build atom cavities with a downward force much stronger than gravity so that atoms can be stored in a single mode of the matter wave. One recently proposed idea is an extension of the magnetic mirror, based on the magnetic uncoupling of hyperfine structure (Hinds *et al.* 1998). We call this device a Zeeman effect surface trap (ZEST).

4. The ZEST: an all-magnetic atom waveguide

The magnetic field of the ZEST is provided once again by a sinusoidally magnetized surface and varies as $B_1 e^{-ky}$. In figure 3, the inset shows the Zeeman shifts in the ground-state hyperfine levels of ^{85}Rb versus magnetic field. The minimum in the hyperfine sublevel $F = 3$, $m_F = -2$, labelled f in figure 3, can be used to trap ^{85}Rb atoms in the direction normal to the mirror at a height where the field strength is $B_{\mathrm{trap}} = 723$ G. The main part of figure 3 illustrates the energies of sub-levels i and f versus distance for a magnetized surface with $\lambda = 1\,\mu$m and $B_1 = 2$ kG. The 'bond length', i.e. the equilibrium position $(\lambda/2\pi)\ln(B_1/B_{\mathrm{trap}})$, is 162 nm from the surface for our particular values. The binding energy is very deep compared with optical dipole force traps and compared with the thermal energy of our laser-cooled atomic cloud (although it is extremely weak in comparison with ordinary physisorption and with molecular binding). The quantized vibration of an atom in this trap has a ground-state width of 9 nm (which is independent of B_1), and a harmonic frequency of 2 MHz (100 μK). The method of coupling atoms into this waveguide is also shown. A conventional cold source, e.g. optical molasses (Lett *et al.* 1989), fires atoms downwards onto the magnetic surface at approximately 1.9 m s^{-1}. On the way, they are optically pumped into the state $i \equiv (F = 2, m_F =$

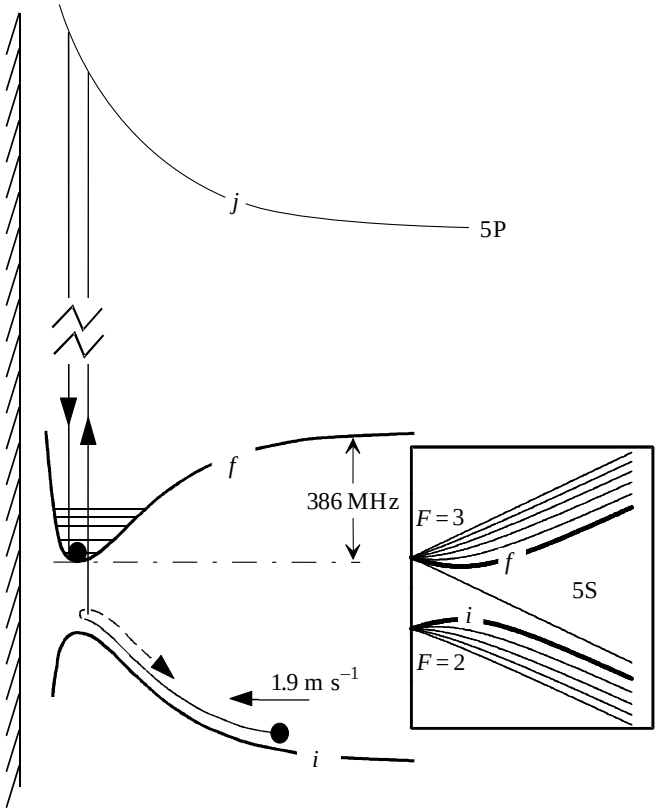

Figure 3. Inset: the Breit–Rabi diagram for ^{85}Rb, showing the Zeeman shifts of the ground-state hyperfine levels drawn to scale. The bold lines show the initial state i of the atoms to be loaded into the waveguide and the final trapped state f. Main diagram: (not to scale) atoms in state i are projected toward the magnetized surface and come to rest at the position of minimum energy for state f, 162 nm from the surface. A laser field couples states i and j, coming into resonance only over a narrow band of positions close to the turning point. The excited atoms decay spontaneously into the trapped state f with a high probability of going into the lowest vibrational mode.

-2). This velocity is chosen so that the atoms come to rest at the maximum of the potential curve, where the energy of state f is a minimum. Here, the Zeeman shift brings the atoms into resonance with a continuous-wave laser beam, which excites state j ($5P_{3/2}, m_j = 3/2, m_I = -5/2$). We have calculated that in field B_{trap}, this state decays spontaneously back to i with 48% probability, and into the bound state f with 52% probability, so, after a small number of excitations, the atoms are all pumped into the waveguide. The region of resonance is only a few nanometres wide because the field gradient, $kB_{\mathrm{trap}} = 45\ \mathrm{G\ nm^{-1}}$, is so strong, and this allows us to introduce atoms into the waveguide in a well-defined region determined by our choice of laser frequency. In particular, it is possible to achieve high coupling efficiency into the $v = 0$ ground state of the waveguide because the width of that state is also a few nanometres. The photons scattered during the loading process do not cause

significant heating of atoms that are already trapped in the waveguide because of the two-dimensional geometry.

To estimate the loading efficiency we have solved the Schrödinger equation for a minimum-uncertainty wave packet initially travelling towards the mirror at 1.9 m s^{-1} in state i. The width of the packet is chosen to be 100 nm; corresponding approximately to the single-photon recoil momentum. The laser field of frequency ω_0 couples states i and j resonantly at 723 G, and state j is allowed to decay outside the i,j system at rate γ. After making the rotating wave approximation and writing the two-component wave function as $\psi(z,t)=(\psi_i,\mathrm{e}^{-\mathrm{i}\omega_0 t}\psi_j)$, the centre-of-mass motion is described by (Garraway & Suominen 1995)

$$\mathrm{i}\hbar\frac{\partial}{\partial t}\begin{pmatrix}\psi_i\\ \psi_j\end{pmatrix}=\begin{pmatrix}T+U_i & V\\ V & T+U_j-\hbar\omega_0-\frac{1}{2}\mathrm{i}\hbar\gamma\end{pmatrix}\begin{pmatrix}\psi_i\\ \psi_j\end{pmatrix}, \tag{4.1}$$

where T is the kinetic energy operator $-(\hbar^2/2m)(\partial^2/\partial y^2)$, U_i and U_j are the potentials shown in figure 3, and V is the transition matrix element. Our solutions to this equation show that we can expect to load atoms into the fundamental mode with an efficiency exceeding 10%. Alternatively, if the waveguide is to be loaded in a single pulse, a second laser can be used to drive the i–j–f Raman transition, and its frequency can be tuned to favour any desired waveguide mode. The disadvantage of this stimulated loading scheme is that atoms already in the trap would be coupled out.

A simple way to detect whether atoms are trapped in the waveguide is to illuminate it with light tuned to the f–j transition: the atoms are then pumped into state i and jump off the surface with a velocity of 1.9 m s^{-1}. With a natural width of 6 MHz, the production spectrum of liberated atoms would not quite resolve the 2 MHz mode spacing, but it would provide an excellent diagnostic tool for the state of atoms in the waveguide. Because of the way the surface is magnetized, the direction $\hat{\boldsymbol{n}}$ of the magnetic field varies with position x according to $\hat{\boldsymbol{n}}=\cos(kx)\hat{\boldsymbol{x}}+\sin(kx)\hat{\boldsymbol{y}}$, imposing an adiabatic spin rotation on the gas as it propagates through the waveguide in the x-direction but not in the z-direction. The associated geometric phase causes an unusual anisotropy in the quantum propagation of the gas, the consequences of which we are currently investigating. The study of two-dimensional gas in the waveguide is not restricted to travelling waves; with a curved magnetic substrate, a depth of 1 mm is sufficient to contain ^{85}Rb up to 14 cm s^{-1}, speeds much greater than we would expect. It will also be possible to contour the waveguide, either physically or by recording a suitable magnetic pattern, so that the 723 G surface has channels, making a kind of 'printed circuit' with paths along which the atoms must flow if they are slow enough.

5. Combined electric–magnetic traps and prospects for atom manipulation

It would be very interesting to increase the phase space density of atoms in the ZEST to the point where the de Broglie wavelength is comparable with the interatomic spacing and quantum statistical effects become important. It is not known at what point relaxation will limit the density of the two-dimensional gas, but the strongest loss mechanism is expected to be spin exchange, in which two $F=3$, $m_F=-2$ atoms collide and emerge in the states $F=3$, $m_F=-1,-3$. Most

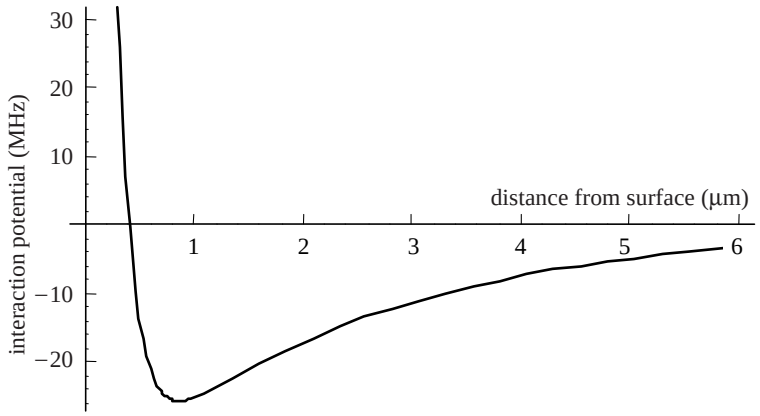

Figure 4. The potential for ^{87}Rb ($F = 2, m_F = 2$) atoms in a combined magnetic–electric two-dimensional trap as a function of distance from the surface. This kind of trap is more suitable than the ZEST for holding atoms at high density, because states of the kind ($F, m_F = F$) are generally more stable against spin-exchange collisions.

probably, the cross-section for this process at 723 G has no particular suppression (F. Abeelen & B. Verhaar, personal communication), and, therefore, Bose–Einstein condensation and related statistical effects are unlikely to be realized in the ZEST. There is, however, another possibility using a combination of static magnetic and electric fields. The idea is to put atoms in the 'stretched' state most strongly repelled from the magnetic mirror: in the case of ^{85}Rb, this is the state $F = 3$, $m_F = 3$, used in § 3 to demonstrate atom focusing. In ^{87}Rb, which is known to form a Bose–Einstein condensate (Griffin *et al.* 1995), it is the state $F = 2$, $m_F = 2$. At the same time as they are magnetically repelled, these atoms can be strongly attracted towards the mirror surface by an electric field gradient. For example, if the electrostatic potential on the surface of the mirror is made to follow $\varphi = \varphi_1 \cos(k_{\mathrm{E}} x)$ (a close analogue of the magnetic mirror), the Laplace equation gives the form $\varphi_1 \cos(k_{\mathrm{E}} x)\mathrm{e}^{-k_{\mathrm{E}} y}$ at height y. Consequently, an atom of static polarizability α, is attracted to the surface by the electrostatic interaction potential

$$U_{\mathrm{E}} = -\tfrac{1}{2}\alpha k_{\mathrm{E}}^2 \varphi_1^2 \mathrm{e}^{-2k_{\mathrm{E}} y}. \tag{5.1}$$

Provided the range $1/k$ of the magnetic repulsion is shorter than the range $1/2k_{\mathrm{E}}$ of this electrostatic attraction, a potential minimum is formed above the surface and the atoms can be trapped in the x–z plane. For example, in figure 4, I show the potential for ^{87}Rb ($F = 2, m_F = 2$) atoms in such a combined electric–magnetic trap along the direction perpendicular to the mirror. At the surface, the magnetic field has a wavelength of 1 μm and a strength of 300 G, while the electric potential has a wavelength of 30 μm and a strength of 15 V. The harmonic frequency of the trap is 90 kHz and the width of the ground-state wave function is 26 nm. This trap is not as stiff as the ZEST (which has a frequency ten times higher), mainly because I have limited the electric field at the surface to 30 kV cm^{-1}, but it would be perfectly adequate to confine a Bose–Einstein condensate of atomic vapour.

Once atoms are held on the surface, it is natural to consider the possibilities for controlled transport. This is particularly appealing in the context of recent ideas in quantum computing (Williams & Clearwater 1998), where coherent superpositions

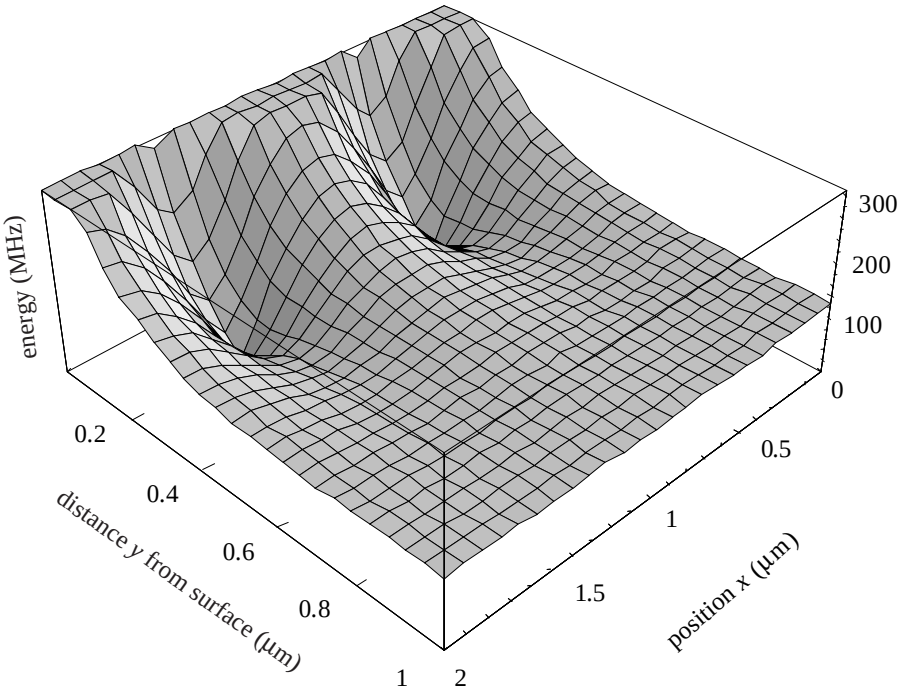

Figure 5. When a uniform magnetic field is added to the two-dimensional trap, the equipotentials are no longer x–z planes. Instead, the atoms are trapped along lines of constant x where the magnetic field of the mirror interferes destructively with the applied field. Atoms captured on these lines can be moved in a controlled way by rotating the applied uniform field.

of atomic states need to be entangled between several atoms in a controlled way. One way to move atoms across the surface involves an additional static magnetic field. If a constant magnetic field $B_0[\cos(\vartheta)\hat{\boldsymbol{x}} + \sin(\vartheta)\hat{\boldsymbol{y}}]$ is superimposed on this trap, the field of the mirror $B_1 \mathrm{e}^{-ky}[\cos(kx)\hat{\boldsymbol{x}} + \sin(kx)\hat{\boldsymbol{y}}]$ interferes constructively with the applied field at positions where $kx = \vartheta$, and destructively at $kx = \vartheta + \pi$. As a result, the equipotentials are no longer plane but exhibit minima as shown in figure 5. Here, the trap parameters are as before, but we have added an 80 G magnetic field along the x-direction. One might also apply a weak magnetic 'holding' field along z in order to avoid having magnetic field zeros where the atoms may undergo Majorana transitions between the magnetic sublevels. In practice, this is probably not necessary because the potential minima in figure 5 are displaced from the magnetic field zeros by the electric force toward the mirror. The atoms are now trapped along lines in the z-direction, spaced $2\pi/k$ apart, and lying approximately 200 nm from the surface. If the angle ϑ of the applied magnetic field is rotated, the potential minima move to new positions where $kx = \vartheta + (2n+1)\pi$. Thus, we have a simple crank to turn that translates the atoms at will along the x-axis by a distance $2\pi/k$ for each rotation of the applied field. At first, one might hope to use the same trick on the sinusoidal electric field, using an applied uniform field to produce pockets in the electrostatic potential. Unfortunately, this does not work because the Stark shift of the ground state is downward. The pockets would have to correspond to local extrema of the electric field and these are forbidden by Gauss's law in the absence of charges.

For quantum computing manipulations, it may be more useful to confine the atoms to dots rather than lines. One approach is to achieve the electrostatic attraction by a row of dots or narrow line segments on the mirror surface, say at $z = z_0$, each of which is charged to the appropriate potential. Now the atoms are constrained electrostatically to move in the x-direction just above the surface at z_0, while being magnetically confined to channels along the z-direction at $kx = \vartheta + (2n+1)\pi$. Even a uniformly charged row of dots is suitable for this purpose because the electric field decreases with height y as a result of the finite width of the dots: we no longer need the sinusoidal boundary potential. This leaves us free to apply a strong potential to some dots and a weaker potential to others, so that when the applied magnetic field is rotated, some atoms will be held in place while others move. This provides a basic mechanism for bringing atoms near to each other and separating them again in a controlled way, so as to produce quantum entanglement. For quantum computing in this way each qubit would be represented by the superposition of two magnetic sublevels in a single ground-state atom. For example, the states might be $|1\rangle \equiv |F = 2, m_F = 2\rangle$ and $|0\rangle \equiv |F = 1, m_F = -1\rangle$ in ^{87}Rb, which are (almost) equally shifted by the electric field but experience magnetic forces that differ by a factor of 2. A single qubit π-flip could be produced by increasing the potential on one of the electrostatic dots so as to pull the atom above that dot into a stronger magnetic field. In the presence of a suitable microwave magnetic field, this would scan the atom through resonance, resulting in an adiabatic interchange of the amplitudes in $|1\rangle$ and $|0\rangle$. Other rotations could be achieved by controlling the duration of the microwave pulse, once again using the electrostatic force to bring a particular atom into resonance with the field. A quantum logic gate operation might be made by holding one atom in place electrostatically, while bringing a neighbouring atom close enough for an interaction to occur. Since the two internal states experience potential barriers of different heights, the coupling will be state-dependent as required.

In this article I have outlined the basic physical principles of the magnetic atom reflector, and have summarized the experimental state of the art. I have also discussed several extensions of the reflector that may be used to confine atoms to a plane, a wire or a dot. These ideas are contributions to the general problem of controlling atomic motion for use in atom optics. In addition, the two-dimensional gas provides an interesting system in which to study quantum statistical properties such as Bose–Einstein condensation and other phase transitions. Finally, I have briefly indicated ways in which one might hope to control individual atoms trapped above a magnetic mirror in order to advance towards the realization of a quantum computer.

It is a pleasure to acknowledge discussions with Peter Zoller, Jörg Schmiedmayer, Rainer Blatt and Richard Hughes. This research was funded by the EPSRC (UK) and the British Council.

References

Adams, C. S. & Riis, E. 1997 Laser cooling and trapping of neutral atoms. *Prog. Quantum Electronics* **21**, 1–79.

Arimondo, E. & Bachor, H. (eds) 1996 Special issue on atom optics. *Quantum Semiclass. Opt.* **8**, 495–753.

Berman, P. R. (ed.) 1997 *Atom interferometry*. San Diego, CA: Academic.

Born, M. & Wolf, E. 1980 *Principles of optics*, 6th edn, p. 303. Oxford: Pergamon.

Garraway, B. M. & Suominen, K. A. 1995 *Rep. Prog. Phys.* **58**, 365–419.

Griffin, A., Snoke, D. W. & Stringari, S. (eds) 1995 *Bose–Einstein condensation*, 1st edn. Cambridge University Press.

Hahn, E. L. 1950 Spin echoes. *Phys. Rev.* **80**, 580–594.

Hinds, E. A., Boshier, M. G. & Hughes, I. G. 1998 Magnetic waveguide for trapping atom gases in two dimensions. *Phys. Rev. Lett.* **80**, 645–649.

Hughes, I. G., Barton, P. A., Roach, T. M., Boshier, M. G. & Hinds, E. A. 1997*a* Atom optics with magnetic surfaces. I. Storage of cold atoms in a curved 'floppy disk'. *J. Phys.* B **30**, 647–658.

Hughes, I. G., Barton, P. A., Roach, T. M. & Hinds, E. A. 1997*b* Atom optics with magnetic surfaces. II. Microscopic analysis of the 'floppy disk' mirror. *J. Phys.* B **30**, 2119–2132.

Jackson, J. D. 1975 *Classical electrodynamics*, 2nd edn, p. 194. New York: Wiley.

Kaenders, W. G., Lison, F., Richter, A., Wynands, R. & Meschede, D. 1995 Imaging with an atomic beam. *Nature* **375**, 214–216.

Lett, P. D., Phillips, W. D., Rolston, S. L., Tanner, C. E., Watts, R. N. & Westbrook, C. I. 1989 Optical molasses. *J. Opt. Soc. Am.* B **6**, 2084–2107.

McClelland, J. J., Schoten, R. E., Palm, E. C. & Celotta, R. J. 1993 Laser-focused atomic deposition. *Science* **262**, 877–880.

Opat, G. I., Wark, J. S. & Cimmino A. 1992 Electric and magnetic mirrors and gratings for slowly moving neutral atoms and molecules. *Appl. Phys.* B **54**, 396–402.

Prentiss, M. G. & Phillips, W. D. (eds) 1997 *Atom optics*. SPIE Proceedings, no. 2995.

Ramsey, N. F. 1985 *Molecular beams*. Oxford University Press.

Roach, T. M., Abele, H., Boshier, M. G., Grossman, H. L., Zetie, K. P. & Hinds, E. A. 1995 Realization of a magnetic mirror for cold atoms. *Phys. Rev. Lett.* **75**, 629–632.

Stern, O. & Gerlach, W. 1922 *Z. Phys.* **8**, 110–111.

Timp, G., Behringer, R. E., Tennant, D. M., Cunningham, J. E., Prentiss, M. & Berggren, K. K. 1992 Using light as a lens for submicron, neutral-atom lithography. *Phys. Rev. Lett.* **69**, 1636–1639.

Wallis, H., Dalibard, J. & Cohen-Tannoudji, C. 1992 Trapping atoms in a gravitational cavity. *Appl. Phys.* B **54**, 407–413.

Williams, C. P. & Clearwater, S. H. 1998 *Explorations in quantum computing*. New York: Springer.

PHILOSOPHICAL TRANSACTIONS OF THE ROYAL SOCIETY A MATHEMATICAL, PHYSICAL & ENGINEERING SCIENCES